Available online at www.sciencedirect.com
SCIENCE DIRECT®
Journal of Luminescence 101 (2003) 211–218
JOURNAL OF LUMINESCENCE
www.elsevier.com/locate/jlumin

Direct nanosecond Nd→Ce nonradiative energy transfer in cerium trifluoride laser crystals

Yu.V. Orlovskii[a,*], T.T. Basiev[a], E.O. Orlovskaya[a], Yu.S. Privis[a], V.V. Fedorov[b], S.B. Mirov[b]

[a] *Laser Materials and Technology Research Center of General Physics Institute RAS, 38 Vavilov st., bld D, 119991, GSP-1, Moscow, Russia*

[b] *The University of Alabama at Birmingham, 1300 University Boulevard, Birmingham, AL 35294-1170, USA*

Received 29 April 2002; received in revised form 12 August 2002; accepted 1 September 2002

Abstract

Using third harmonics of $LiF:F_2^+$ tunable color center laser excitation and selective fluorescence detection the temperature and concentration dependencies of fluorescence decay curves of the high-lying $^4D_{3/2}$ manifold of the Nd^{3+} ion were measured in CeF_3 crystals. As a result the temperature dependence of energy transfer kinetics from the $^4D_{3/2}$ manifold of the Nd^{3+} donor ions to the $^2F_{7/2}$ manifold of the acceptor Ce^{3+} ions in the ordered practically 100% filled CeF_3: Nd^{3+} (0.056 wt%) crystal lattice was determined for 13–55 K. Based on the temperature dependence the mechanisms and the channels of the Nd→Ce nonradiative energy transfer have been recognized. The net growth of the resonance Nd→Ce energy transfer rate in the temperature range from 25 to 55 K is found to be almost 3 orders of magnitude from 9.0×10^4 to 2.84×10^7 s^{-1}.

In a CeF_3: Nd^{3+} (0.63 wt%) crystal a significant contribution of the Nd→Nd resonance energy transfer to the $^4D_{3/2}$ manifold quenching is found for 20–40 K and its channel and mechanism are suggested.

Discussion of the possibility of subpicosecond and picosecond nonradiative energy transfer in rare-earth doped laser crystals is provided.

PACS: 71.70.Ch; 78.47.+p

Keywords: CeF_3: Nd^{3+}; Nanosecond; Nonradiative energy transfer

1. Introduction

In Refs. [1–3] a nanosecond quenching energy transfer of high-lying strongly quenched by the multiphonon relaxation the $^4G_{7/2}+{}^2K_{13/2}$ manifold of the Nd^{3+} ion have been investigated in LaF_3 crystals. Experimentally measured kinetics of energy transfer was well described accounting the sum of dipole–dipole ($s=6$) and dipole–quadrupole ($s=8$) interactions between donors and acceptors. The abnormally high microefficiencies of the Nd–Nd quenching $C_{DA}^{(6)} = 0.5 \times 10^{-37}$ cm^6/s and $C_{DA}^{(8)} = 2.5 \times 10^{-51}$ cm^8/s were found for 77 K [2,3]. Accounting the sum over

*Corresponding author. Tel.: +7-095-1328376; fax: +7-095-1350270.

E-mail address: orlovski@lst.gpi.ru (Yu.V. Orlovskii).

0022-2313/02/$ - see front matter
PII: S0022-2313(02)00437-4

all the sites of the acceptor sublattice the quenching rate for the so-called ordered stage of kinetics decay and additive contribution of two interaction mechanisms can be given by (see, for example, Ref. [1])

$$W = c_A\left(C_{DA}^{(6)}\sum_n R_n^{-6} + C_{DA}^{(8)}\sum_n R_n^{-8}\right), \qquad (1)$$

where c_A is the relative concentration of acceptors, and R_n is the distance between donor and nth acceptor. For a LaF_3 crystal the lattice sums $\sum_n R_n^{-6} = 2.44\times10^{-3}$ A^{-6} and $\sum_n R_n^{-8} = 1.20\times10^{-4}$ A^{-8} have been calculated in Refs. [1–3]. For small concentration of excited donors and the ordered 100% filled NdF_3 crystal lattice ($c_A \cong 1$) this gives the Nd–Nd energy transfer rate $W = 3.12\times10^9$ s^{-1} or energy transfer characteristic time $\tau = 320$ ps. To understand if such picosecond rates of direct energy transfer between rare-earth ions in the ordered crystals are normal or abnormal and to determine the mechanism of fast ion–ion interaction the model system with simple energy level scheme of acceptor ions supposed limited number of channels of inter-multiplet cross-relaxation of excited state of donor (Nd^{3+}) and unexcited state of acceptor (Ce^{3+}) ions was chosen. Because the lattice is 100% ordered and filled this makes the energy transfer kinetics pure exponential and easy for analysis. Also, limited number of channels of inter-multiplet cross-relaxation makes the temperature dependence analysis simpler. To make the contribution of Nd–Nd energy transfer negligible one can decrease the concentration of the Nd^{3+} ions and thus to measure the Nd–Ce energy transfer rate directly.

2. Experimental techniques

Two crystals of CeF_3: Nd^{3+} (0.63 wt%) and CeF_3: Nd^{3+} (0.056 wt%) were grown by Bridgman–Stockbarger technique in fluorinating atmosphere. The concentrations of Nd^{3+} were determined by microprobe X-ray analysis on a Camebax system. For a fluorescence excitation solid state tunable $LiF:F_2^{+**}$ laser pumped by an alexandrite laser (Light Age, Inc.) [4] was used. The basic Q-switched alexandrite laser provides tunable radiation in 720−810 nm spectral range with 200 mJ pulse energy and 10−26 Hz repetition rate. The $LiF:F_2^{+**}$ laser cavity was based on Littrow configuration consisting of an input dichroic mirror and a plane diffraction grating (1200 g/mm). The $LiF:F_2^{+**}$ active element was Brewster cut with a length of 4 cm. Its absorption coefficient at 740 nm was 1.2 cm^{-1}. The $LiF:F_2^{+**}$ laser exhibits good photo and thermostable operation at room temperature when pumped by an alexandrite laser and can provide efficient high power lasing tunable in 800−1200 nm spectral range. The $LiF:F_2^{+**}$ pulses had duration of 60 ns at 0.15 of maximum intensity and 35 ns at the half of it. The fall time of the laser pulse was 17 ns, which allowed to measure correctly the decay time longer than 30 ns. The spectral width of laser pulse was 0.2 cm^{-1}. Tunable visible (400−600 nm) and UV (300−400 nm) radiations were achieved by second and third harmonics of $LiF:F_2^{+**}$ color center laser in a BBO nonlinear crystals (10 mm × 4 mm × 7 mm). For the fluorescence selection and registration ARC-750 spectrometer and R928 Hamamatsu PMT were used. Signal acquisition, recording and treatment was provided by Tektronix TDS-380 (350 MHz bandwidth) digital averaging oscilloscope and Boxcar-Integrator SR250 (Stanford Research System) linked with PC. The closed-cycle Janis cryostat with temperature controller was used for CeF_3: Nd^{3+} crystals cooling in the range from 13 to 55 K.

In order to select the best fluorescent transition for kinetic measurements the fluorescence spectrum of a CeF_3: Nd^{3+} (0.63 wt%) crystal for 330 nm excitation into the $^4D_{7/2}$ manifold at $T = 15$ K was measured. Because of small energy gap between $^4D_{7/2}$ and $^4D_{3/2}$ manifolds ($\Delta E = 500$ cm^{-1}), exited ions relax to the $^4D_{3/2}$ manifold via one- or two-phonon relaxation process with relaxation time less than 1 ns. Three spectral bands belong to the $^4D_{3/2}\rightarrow{}^4I_{9/2}$; $^4I_{11/2}$; $^4I_{13/2}$ transitions were observed (Fig. 1). The fluorescence of the strongest $^4D_{3/2}\rightarrow{}^4I_{11/2}$ transition can be mixed with the fluorescence of the metastable $^2P_{3/2}$ manifold at the $^2P_{3/2}\rightarrow{}^4I_{9/2}$ transition and

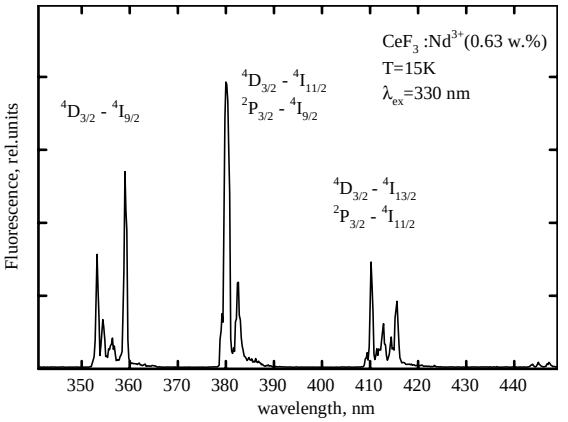

Fig. 1. Fluorescence spectra of the CeF_3: Nd^{3+} (0.63 wt%) crystal for 330 nm excitation at $T = 15$ K.

fluorescence of the $^4D_{3/2} \rightarrow {}^4I_{13/2}$ transition can be mixed with the $^2P_{3/2} \rightarrow {}^4I_{11/2}$ one. Therefore, to avoid emission spectra overlap all fluorescence kinetic measurements were done for the resonance $^4D_{3/2} \rightarrow {}^4I_{9/2}$ transition at 352.8 nm excitation and 359 nm detection wavelengths.

3. Results and discussion

3.1. Nd–Ce energy transfer

The fluorescence kinetics of the $^4D_{3/2}$ manifold in both CeF_3: Nd^{3+} crystals show pure exponential behavior for all the temperatures. The measured decay times are presented in Table 1. The measured decay times were found much shorter than that measured in LaF_3: Nd^{3+} (0.005 wt%) in Ref. [5] ($\tau = 35$ μs). For a CeF_3: Nd^{3+} (0.63 wt%) crystal smaller lifetimes than those for a CeF_3: Nd^{3+} (0.056 wt%) crystal were measured in the temperature range from 20 to 40 K. But for $T = 13.6$ K and $T > 40$ K the measured lifetimes for both concentrations of Nd^{3+} are found to be equal.

First, the Nd–Ce energy transfer was analyzed. In doing so, an assumption was made that contribution of the Nd–Nd energy transfer to the $^4D_{3/2}$ manifold quenching is negligible for CeF_3: Nd^{3+} (0.056 wt%) crystal with very small concentration of Nd^{3+}. Also suppose that the intra-center relaxation rate of the $^4D_{3/2}$ manifold does not change significantly from LaF_3: Nd^{3+} to CeF_3: Nd^{3+} and it can be calculated from the measured in Ref. [5] the decay time τ of the $^4D_{3/2}$ manifold in a LaF_3: Nd^{3+} (0.005 wt%) crystal ($W_{\text{int.}} = 1/\tau = 2.86 \times 10^4$ s^{-1}). It is an experimentally established fact that multiphonon relaxation (MR) rate practically does not depend on the temperature in the range from 0 to 77 K. Hence, the Nd–Ce energy transfer rate can be calculated as $W_{\text{Nd-Ce}}(T) = W_{\text{meas.}}(T) - W_{\text{int.}}$. Fig. 2 shows temperature dependence of the Nd–Ce energy transfer rate in the CeF_3: Nd^{3+} crystals. As one can see in the temperature range from 13 to 20 K the measured relaxation rate was not changed ($W = 1.5 \times 10^5$ s^{-1}). Then strong increase of the relaxation rate from $W = 1.5 \times 10^5$ s^{-1} at 20 K to $W = 1.4 \times 10^7$ s^{-1} at 55 K was observed. In order to clarify the temperature-dependent channel of the Nd–Ce energy transfer, the difference $W(T) - W(13\text{ K})$ was studied. The temperature dependent channel of Nd–Ce energy transfer with the following cross-relaxation transitions $\{^4D_{3/2}(2') \rightarrow {}^2P_{3/2}(1)$ and $^2F_{5/2}(2) \rightarrow {}^2F_{7/2}(1')\}$ with activation energy $\Delta E = 207$ cm^{-1} and small energy mismatch $\varepsilon = 29$ cm^{-1} can be considered as a main candidate for the of Nd–Ce energy transfer in the 20−77 K temperature range (Fig. 3). For a multipole ion–ion interaction the temperature dependence of the energy transfer rate $W^{ij}_{\text{DA}}(T)$ for resonance mechanism can be presented by the

Table 1
The measured decay times of the $^4D_{3/2}$ manifold versus temperature in CeF_3 crystals for different concentrations of Nd^{3+}

T (K)	13.6	20.4	25.4	30.4	35.6	40.8	45.8	50.8	55.6
τ (μs) 0.056 wt%	6.5	6.5	4.1	1.9	0.6	0.26	0.11	0.07	—
τ (μs) 0.63 wt%	6.5	4.1	1.9	0.75	0.35	0.17	0.11	0.07	0.035

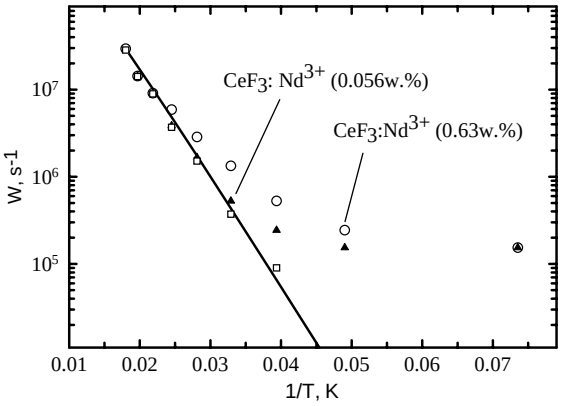

Fig. 2. The measured energy transfer rates versus $1/T$ in the CeF_3: Nd^{3+}(0.63 wt%) crystal—open circles; in the CeF_3: Nd^{3+} (0.056 wt%) crystal—filled triangles; the rate of the Nd–Ce resonance energy transfer ($W_{res.}$) in CeF_3: Nd^{3+} (0.056 wt%) calculated as $W_{res.}(\mathrm{Nd-Ce}) = \tau(T)^{-1} - \tau^{-1}(13\ \mathrm{K})$—open rectangles, and the product of Boltzmann populations of the second CF level of the $^4D_{3/2}$ excited manifold of donors (Nd^{3+}) and the second CF level of the ground $^2F_{5/2}$ manifold of acceptors (Ce^{3+}) ($n_D(E_2,T)n_A(E_2,T)$) (see Fig. 3 for energy levels diagram) normalized to the measured Nd–Ce energy transfer rate for $T = 55$ K—solid line.

following equation:

$$W_{DA}^{i'j}(T) = n_D(E_{i'},T)n_A(E_j,T)\frac{C_{DA}^{i'j(s)}(T)}{R^s}, \qquad (2)$$

where $n_D(E_{i'},T)$ is Boltzmann population of i'th crystal field (CF) level of donor excited manifold at specific temperature and $n_A(E_j,T)$ is that of jth CF level of acceptor ground manifold; $C_{DA}^{i'j(s)}$ is the partial microefficiency of energy transfer determined by the partial overlap integral of donor fluorescence and acceptor absorption spectra for inter-CF transitions ($s = 6$ for dipole–dipole, 8 for dipole–quadrupole, 10 for quadrupole–quadrupole, etc.). The value of ε in the measured temperature range can be comparable with the spectral line width of above mentioned $2\to1$ transitions providing non-zero overlap integral.

The thermal stimulation of resonance Nd–Ce energy transfer rate can be compared with the product of Boltzmann populations of the second CF level of the $^4D_{3/2}$ excited manifold of donors (Nd^{3+}) and the second CF level of the ground manifold of acceptors (Ce^{3+}) ($W(T)$ (Nd−Ce)$\sim n_D(E_{2'},T)n_A(E_2,T)$) normalized to the measured

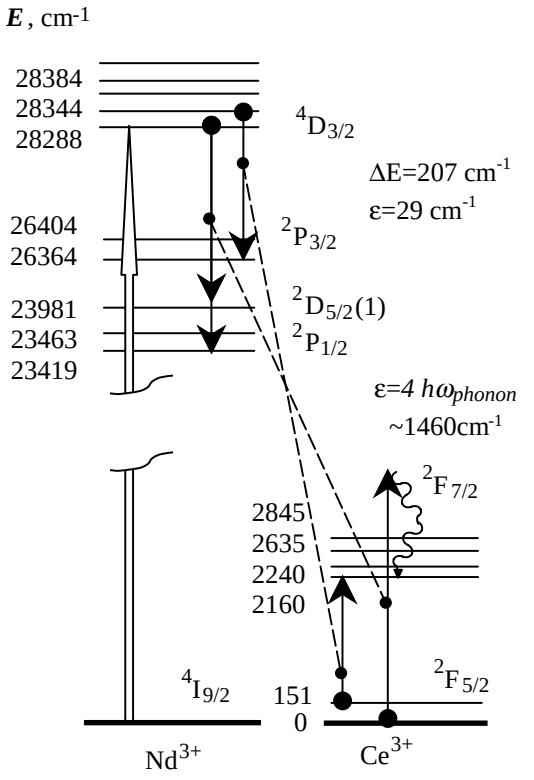

Fig. 3. Energy scheme of the Nd–Ce nonradiative quenching energy transfer in a CeF_3 crystal.

Nd–Ce energy transfer rate for $T = 55$ K. Rather good fit with the measured values for the temperature range 25−50 K was obtained (Fig. 2). Also, an activation energy of the temperature stimulation of the Nd–Ce energy transfer process can be found from the slope of the measured temperature dependence ($\ln W(T) = \ln W_1 - \Delta E/k(1/T)$) which is equal to $\Delta E = 207\ \mathrm{cm}^{-1}$. It is determined by $n_D(E_{2'},T)$ with $\Delta E = 56\ \mathrm{cm}^{-1}$ and $n_A(E_2,T)$ with $\Delta E = 151\ \mathrm{cm}^{-1}$.

For the temperatures lower than 25 K large difference between the measured Nd–Ce energy transfer rate and the theoretical model is seen (Fig. 2). For $T\to0$ contribution of the resonance channel described above is negligible. Therefore, another mechanism should be considered for low temperatures, e.g. phonon-assisted energy transfer with emission of at least four phonons ($\hbar\omega_{\mathrm{eff.}} \cong 365\ \mathrm{cm}^{-1}$) to compensate $1462\ \mathrm{cm}^{-1}$

energy difference for the $\{^4D_{3/2}(1) \rightarrow {}^2D(1)_{5/2}$ and $^2F_{5/2}(1) \rightarrow {}^2F_{7/2}(4')\}$ cross-relaxation transitions (Fig. 3). There is no thermal stimulation for this mechanism in the measured temperature range, which can be estimated in the single-frequency model of crystal lattice vibrations using the following equations [6]:

$$W_{\text{ph.ass.tr.}}(T) = W_0(n(\omega, T) + 1)^n, \quad (3)$$

$$n(\omega, T) = (\exp(h\omega_{\text{eff.}}/kT) - 1)^{-1}, \quad (4)$$

where W_0 is the phonon assisted energy transfer rate at $T = 0$ K (it can be considered as a spontaneous energy transfer rate), n is the number of phonons involved in the process; $n(\omega, T)$ is the population of a phonon mode of frequency ω at a temperature T described by the Bose–Einstein distribution. The effective optical phonon for LaF_3 and CeF_3 crystals can be varied from 350 to 400 cm^{-1}. In accordance with Eqs. (3) and (4) the thermal stimulation of the Nd–Ce energy transfer rate in the temperature range from 13 to 77 K can be considered as a constant (W_0). The Nd–Ce energy transfer rate from phonon-assisted energy transfer with four phonon emission can be calculated using the following $W_0 = 1/\tau_{\text{meas.}}(13\text{ K}) - W_{\text{int.}} = 1.25 \times 10^5$ s^{-1} ($\tau_{\text{tr.}} = 8$ μs).

Thereby, it is found that at $T = 13$ K a four phonon assisted Nd–Ce energy transfer together with intra-center relaxation provides fluorescence quenching of the $^4D_{3/2}$ manifold. But at $T = 30$ K its rate is already lower than the rate of resonance Nd–Ce energy transfer (see Table 2). Starting from 35 K the resonance Nd–Ce energy transfer is dominated in the CeF_3: Nd^{3+} (0.056 wt%) crystal. A 315 times net growth of the rate of resonance Nd–Ce energy transfer in the temperature range from 25 to 55 K is found. This is equivalent to the fall of the Nd→Ce resonance energy transfer characteristic time from 11.1 μs at 25 K to 35 ns at 55 K. If we extrapolate the fitting curve in Fig. 2 to 77 K the energy transfer rate obtained will be $\sim 10^8$ s^{-1} or τ_{tr} will be equal to 10 ns. But even this nanosecond characteristic time is ~30 times slower than the Nd–Nd energy transfer characteristic time of the $^4G_{7/2}$ manifold in the NdF_3 crystal at 77 K ($\tau_{\text{tr.}} = 320$ ps). The total Nd→Ce energy transfer rate in CeF_3 crystals from the $^4D_{3/2}$ manifold for small concentrations of the Nd^{3+} ions may be roughly estimated using equation $W(T) = W_0 + W_1 \exp(-\Delta E/kT)$, with parameters $W_0 = 1.25 \times 10^5$ s^{-1}, $W_1 = 6 \times 10^9$ s^{-1} and $\Delta E = 207$ cm^{-1}. It is seen that for $\Delta E \ll kT$ the Nd–Ce resonance energy transfer characteristic time may come up to subpicosecond level ($\tau_{\text{tr.}} = 1/W_1 = 160$ ps) even for small and zero reduced matrix elements of the $^4D_{3/2} \rightarrow {}^2P_{3/2}$ transition in donor ($(U^{(2)})^2 = 0.0118$, $(U^{(4)})^2 = 0$, $(U^{(6)})^2 = 0$ [7]). The energy transfer characteristic time of self-quenching of the $^4G_{7/2}$ manifold of Nd^{3+} by two $^4G_{7/2}(2)$; $^4I_{9/2}(2) \rightarrow {}^4G_{5/2} + {}^2G_{7/2}(1)$; $^4I_{11/2}(1)$ visible and mid IR cross-relaxation channels ($\Delta E = 132$ cm^{-1}, $\varepsilon = 5$ cm^{-1}) estimated at $\Delta E \ll kT$ for NdF_3 crystal exceeds 30 ps. But here the reduced matrix elements for $^4G_{7/2} \rightarrow {}^4G_{5/2} + {}^2G_{7/2}$ and $^4G_{7/2} \rightarrow {}^4I_{11/2}$ transitions in donor are much higher ($(U^{(2)})^2 = 0.0575$, $(U^{(4)})^2 = 0.2251$, $(U^{(6)})^2 = 0.088$ and $(U^{(2)})^2 = 0.6273$, $(U^{(4)})^2 = 0.0959$, $(U^{(6)})^2 = 0.0120$, respectively). So, some correlation between the subpicosecond and picosecond energy transfer characteristic times and reduced matrix elements of electronic transitions involved is observed.

Table 2
The rate of the Nd–Ce resonance energy transfer ($W_{\text{res.}}$) in CeF_3: Nd^{3+} (0.056 wt%) calculated as $W_{\text{res.}}(\text{Nd}-\text{Ce}) = \tau(T)^{-1} - \tau^{-1}$ (13 K), and the rate of Nd–Nd energy transfer ($W(\text{Nd}-\text{Nd})$) calculated as $W(\text{Nd}-\text{Nd}) = \tau(T)^{-1}$ (0.63 wt%) $- \tau(T)^{-1}$ (0.056 wt%)

T (K)	$W_{\text{res.}}(\text{Nd}-\text{Ce}) = \tau(T)^{-1} - \tau^{-1}$ (13 K)	$W(\text{Nd}-\text{Nd}) = \tau(T)^{-1}$ (0.63 wt%) $- \tau(T)^{-1}$ (0.056 wt%)
13.6	0	0
20.4	0	9.0×10^4
25.4	9.0×10^4	2.9×10^5
30.4	3.73×10^5	8.07×10^5
35.6	1.513×10^6	1.191×10^6
40.8	3.692×10^6	2.036×10^6
45.8	8.937×10^6	
50.8	1.4132×10^7	
55.6	2.842×10^7	

3.2. Nd–Nd energy transfer

The temperature dependence of the Nd–Nd energy transfer rates from the $^4D_{3/2}$ manifold can

be obtained from the measurements of decay times in CeF_3: Nd^{3+} (0.63 wt%) crystal with 10 times higher concentration of Nd^{3+} ions. The Nd–Nd energy transfer rates can be simply calculated as a difference between the measured decay rates in CeF_3: Nd^{3+} (0.63 wt%) and CeF_3: Nd^{3+} (0.056 wt%) crystals ($W(\mathrm{Nd-Nd}) = \tau(T)^{-1}$ (0.63 wt%) $- \tau(T)^{-1}$ (0.056 wt%)) (Table 2). The thermal stimulation of the Nd–Nd energy transfer rate can be compared with the product of Boltzmann populations of the second CF level ($\Delta E = 56\ \mathrm{cm}^{-1}$) of the $^4D_{3/2}$ excited manifold of the Nd^{3+} donors and the lowest CF level of the ground $^4I_{9/2}$ manifold ($\Delta E = 0$) of the Nd^{3+} acceptors ($W(T)(\mathrm{Nd-Nd}) \sim n_D(E_{2'}, T) n_A(E_1, T)$) (see Fig. 4 for energy levels diagram) normalized to the measured energy transfer rate for $T = 20$ K (solid line in Fig. 5). The energy mismatch ε for the respective cross-relaxation transitions in the IR $\{^4D_{3/2}(2') \rightarrow {}^2P_{3/2}(1);\ {}^4I_{9/2}(1) \rightarrow {}^4I_{11/2}(1)\}$ and the visible $\{^4D_{3/2}(2') \rightarrow {}^4I_{11/2}(1);\ {}^4I_{9/2}(1) \rightarrow {}^2P_{3/2}(1)\}$

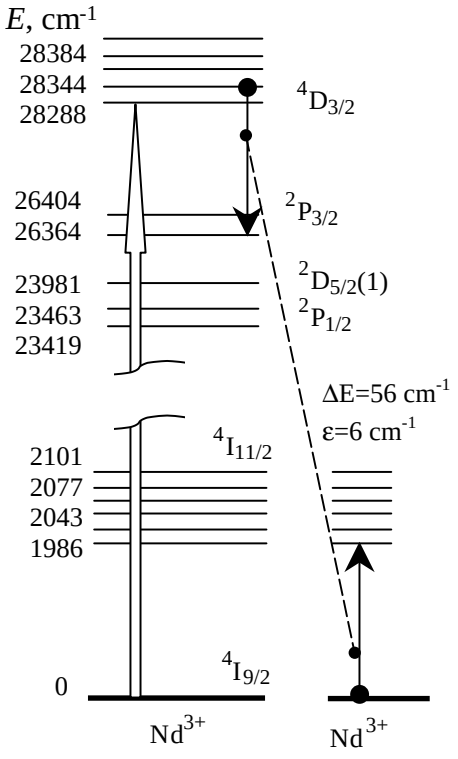

Fig. 4. Energy scheme of the Nd–Nd nonradiative self-quenching in a CeF_3 crystal.

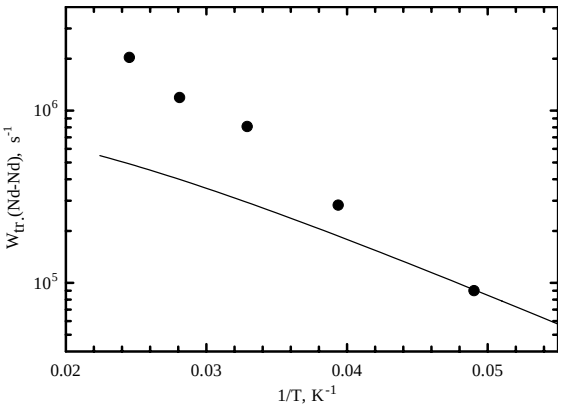

Fig. 5. The Nd–Nd nonradiative energy transfer rates versus temperature calculated as $W(\mathrm{Nd-Nd}) = \tau(T)^{-1}$ (0.63 wt%) $- \tau(T)^{-1}$ (0.056 wt%)-filled circles, and the product of Boltzmann populations of the second CF level of the $^4D_{3/2}$ excited manifold of donors (Nd^{3+}) and the lowest CF level of the ground $^4I_{9/2}$ manifold of acceptors (Nd^{3+}) ($n_D(E_2, T) n_A(E_1, T)$) (see Fig. 4 for energy levels diagram) normalized to the measured energy transfer rate for $T = 20$ K—solid line.

spectral ranges is equal to $6\ \mathrm{cm}^{-1}$. A resonance energy transfer can be easily provided by this channel. The contribution of a cross-relaxation channel in the visible spectral range seems to be negligible because of much smaller reduced matrix elements $U^{(k)}$ of visible absorption $^4I_{9/2} \rightarrow {}^2P_{3/2}$ transition ($(U^{(2)})^2 = 0$, $(U^{(4)})^2 = 0.0014$, $(U^{(6)})^2 = 0.0008$) in comparison with the IR $^4I_{9/2} \rightarrow {}^4I_{11/2}$ one ($(U^{(2)})^2 = 0.0195$, $(U^{(4)})^2 = 0.1073$, $(U^{(6)})^2 = 1.1653$). As one can see the measured values of Nd–Nd energy transfer rates lie higher than the constructed curve for the temperatures higher than 20 K. It may be attributed to an increase of microefficiency of energy transfer ($C_{DA}^{ij}(T)$) (see Eq. (2)) from an increase of overlap integral with temperature [8].

Thereby, in 20–40 K temperature range significant contribution of the Nd→Nd energy transfer to $^4D_{3/2}$ quenching by resonance mechanism was found in a CeF_3: Nd^{3+} (0.63 wt%) crystal. Also, it is found that at $T = 20$ K in the CeF_3: Nd^{3+} (0.63 wt%) crystal the contribution of resonance the Nd–Nd energy transfer to the $^4D_{3/2}$ manifold quenching is comparable with phonon assisted the Nd–Ce energy transfer. At 25 K all three energy transfer processes: phonon

assisted Nd–Ce energy transfer with 4 phonon emission, the Nd–Ce and the Nd–Nd resonance energy transfer have comparable contributions to the $^4D_{3/2}$ manifold quenching. At $T = 30$ K the resonance quenching Nd–Nd energy transfer is dominated. Because concentration of the Nd^{3+} acceptors is 2 orders of magnitude lower than Ce^{3+} one can conclude that at 30 K the efficiency of resonance Nd–Nd energy transfer is more than 2 orders of magnitude higher than the Nd–Ce energy transfer. Starting from 30 K the resonance Nd–Ce energy transfer rate growths faster than that Nd–Nd. This is evident from strong increase with the temperature of population of the second lowest Stark (CF) level of the ground $^2F_{5/2}$ manifold of the Ce^{3+} acceptors and decrease of population of the lowest Stark level of the ground $^4I_{9/2}$ manifold of the Nd^{3+} acceptors. As a result at 45 K the contribution of the Nd–Nd resonance energy transfer to the $^4D_{3/2}$ manifold quenching becomes negligible in comparison with the Nd–Ce resonance energy transfer even in the CeF_3: Nd^{3+} (0.63 wt%) crystal with relatively high concentration of Nd^{3+}. However, for $\Delta E \ll kT$ rough estimation of the Nd–Nd energy transfer characteristic time from the $^4D_{3/2}$ manifold in the NdF_3 crystal gives subpicosecond value. Alternatively, estimated for $\Delta E \ll kT$ from results of Ref. [9] the energy transfer characteristic time of the $^4F_{3/2}$ metastable state self-quenching in the NdF_3 crystal by the $^4F_{3/2}(2)$; $^4I_{9/2}(1) \rightarrow {}^4I_{15/2}(1)$; $^4I_{15/2}(1)$ IR cross-relaxation channel ($\Delta E = 42\ cm^{-1}$, $\varepsilon = 3\ cm^{-1}$) do not exceed microsecond value. But this channels have mostly zero or very small reduced matrix elements for both the $^4F_{3/2} \rightarrow {}^4I_{15/2}$ ($(U^{(2)})^2 = 0$, $(U^{(4)})^2 = 0$, $(U^{(6)})^2 = 0.0288$) transition in donor and the $^4I_{9/2} \rightarrow {}^4I_{15/2}$ ($(U^{(2)})^2 = 0$, $(U^{(4)})^2 = 0.0001$, $(U^{(6)})^2 = 0.0453$) transition in acceptor. This result confirms correlation between the energy transfer characteristic times and reduced matrix elements $U^{(k)}$ of electronic transitions involved.

4. Conclusion

Based on the measured temperature dependence mechanisms and channels of the Nd→Ce non-radiative energy transfer have been proposed for the CeF_3: Nd^{3+} crystals. At 13 K the relaxation rate of the $^4D_{3/2}$ manifold is determined only by intra-center relaxation and phonon-assisted energy transfer with four-phonon emission $\{^4D_{3/2} \rightarrow {}^2D(1)_{5/2}$ and $^2F_{5/2}(2) \rightarrow {}^2F_{7/2}(4')\}$. In the CeF_3: Nd^{3+} (0.056 wt%) crystal the resonance mechanism of Nd–Ce energy transfer by the $\{^4D_{3/2}(2') \rightarrow {}^2P_{3/2}(1)$ and $^2F_{5/2}(2) \rightarrow {}^2F_{7/2}(1')\}$ cross-relaxation transitions with $\Delta E = 207\ cm^{-1}$ and the energy mismatch $\varepsilon = 29\ cm^{-1}$ is dominated for the temperatures higher than 30 K. The net growth of the resonance Nd→Ce energy transfer rate in the temperature range from 25 to 55 K is found to be almost 3 orders of magnitude from 9.0×10^4 to $2.84 \times 10^7\ s^{-1}$. Analysis of the measured temperature dependence shows that for $\Delta E \ll kT$ the Nd–Ce resonance energy transfer characteristic time may come up to subpicosecond level ($\tau_{tr.} = 1/W_1 = 160$ ps). On the other hand, the energy transfer characteristic time of self-quenching of the $^4G_{7/2}$ manifold of Nd^{3+} by two $^4G_{7/2}(2)$; $^4I_{9/2}(2) \rightarrow {}^4G_{5/2} + {}^2G_{7/2}(1)$; $^4I_{11/2}(1)$ visible and mid IR cross-relaxation channels with $\Delta E = 132\ cm^{-1}$ and $\varepsilon = 5\ cm^{-1}$ estimated at $\Delta E \ll kT$ for NdF_3 crystal exceeds 30 ps. Higher picosecond rate of energy transfer in the later case correlates well with the larger reduced matrix elements of electronic transitions in donor in comparison with the Nd–Ce subpicosecond energy transfer. Nevertheless, it is found that in the ordered crystals the subpicosecond rates of energy transfer can be realized even for small and zero reduced matrix elements $U^{(k)}$ of donor electronic transitions.

In a CeF_3: Nd^{3+} (0.63 wt%) crystal a significant contribution of the Nd→Nd resonance energy transfer to the $^4D_{3/2}$ manifold quenching by the $\{^4D_{3/2}(2') \rightarrow {}^2P_{3/2}(1)$; $^4I_{9/2}(1) \rightarrow {}^4I_{11/2}(1)\}$ intermultiplet Stark–Stark cross-relaxation transitions lying in the IR spectral range with $\Delta E = 56\ cm^{-1}$ and the energy mismatch $\varepsilon = 6\ cm^{-1}$ is found for 20−40 K. At 45 K the contribution of Nd→Ce nanosecond resonance energy transfer to the total $^4D_{3/2}$ manifold decay becomes dominated in this crystal, too.

Also, for $\Delta E \ll kT$ the energy transfer characteristic time of subpicosecond value for the Nd–Nd

energy transfer from the $^4D_{3/2}$ manifold is estimated for NdF_3 crystal. Alternatively, estimated for $\Delta E \ll kT$ the energy transfer characteristic time of the $^4F_{3/2}$ metastable state self-quenching in the NdF_3 crystal by the $^4F_{3/2}(2)$; $^4I_{9/2}(1) \rightarrow {}^4I_{15/2}(1)$; $^4I_{15/2}(1)$ IR cross-relaxation channel ($\Delta E = 42\ cm^{-1}$, $\varepsilon = 3\ cm^{-1}$) do not exceed microsecond value, which correlates with zero and small values of reduced matrix elements of both donor and acceptor electronic transitions involved into energy transfer.

Acknowledgements

This work was partially supported by NSF grants ECS-9710428 and ECS-0140484, Ligth Age, Inc. Agreement and DoD/BMDO/SBIR project #DASG60-97-M-0110, RFBR grants 99-02-18212a and 00-02-17108a, grant of Russian Ministry of Industry, Science and Technology on Fundamental Spectroscopy No M-3-02 and the Program of the Government of Russian Federation for Integration of Science and High Education (project No I0821). We'd like also to thank Dr. K.K. Pukhov for fruitful theoretical discussions.

References

[1] T.T. Basiev, Yu.V. Orlovskii, Sov. Phys. JETP 69 (1989) 1109.
[2] T.T. Basiev, Yu.V. Orlovskii, Yu.S. Privis, Fiz. Tverdogo Tela (St. Petersburg) Solid State Phys. 38 (1996) 1023.
[3] T.T. Basiev, Yu.V. Orlovskii, Yu.S. Privis, J. Lumin. 69 (1996) 187.
[4] A.Yu. Dergachev, S.B. Mirov, Opt. Commun. 145 (1998) 107.
[5] M.F. Joubert, B. Jacquier, C. Linares, R.M. Macfarlane, J. Lumin. 53 (1992) 477.
[6] T. Miyakawa, D.L. Dexter, Phys. Rev. B 1 (1970) 2961.
[7] A. Kornienko, Vitebsk State University, Belarus, unpublished.
[8] A.S. Agabekyan, Opt. Spektrosk. 30 (1971) 449.
[9] Yu.K. Voron'ko, T.G. Mamedov, V.V. Osiko, A.M. Prokhorov, V.P. Sakun, I.A. Shcherbakov, Sov. Phys. JETP 71 (1976) 778 (in Russian).